JACS
JOURNAL OF THE AMERICAN CHEMICAL SOCIETY

Article

pubs.acs.org/JACS

Toward a Quantitative Understanding of Symmetry Reduction Involved in the Seed-Mediated Growth of Pd Nanocrystals

Hsin-Chieh Peng,[†] Jinho Park,[†] Lei Zhang,[‡] and Younan Xia*[,†,‡]

[†]School of Chemistry and Biochemistry, Georgia Institute of Technology, Atlanta, Georgia 30332, United States

[‡]The Wallace H. Coulter Department of Biomedical Engineering, Georgia Institute of Technology and Emory University, Atlanta, Georgia 30332, United States

Supporting Information

ABSTRACT: We report a quantitative analysis of the symmetry reduction phenomenon involved in the seed-mediated growth of Pd nanocrystals under dropwise addition of a precursor solution. In addition to the elimination of self-nucleation, the dropwise approach allows for the formation of a steady state for the number of precursor ions in the growth solution, which only fluctuates in a narrow range defined by experimental parameters such as the initial concentration of precursor solution and the injection rate. We can deterministically control the growth mode (symmetric vs asymmetric) of a seed by tuning these parameters to quantitatively manipulate the reaction kinetics and thus the lower and upper limits that define the steady state. We demonstrate that there exists a correlation between the growth mode and the lower limit of precursor ions in the steady state of a seed-mediated growth process. For the first few drops of precursor solution, the resultant atoms will only be deposited on a limited number of available sites on the seed if the lower limit of the steady state is below a critical value. Afterward, the deposition of atoms will be largely confined to these initially activated sites to induce symmetry reduction if atom deposition is kept at a faster rate than surface diffusion by controlling the lower limit of precursor ions in the steady state. Otherwise, the migration of atoms to other regions through surface diffusion can access other sites on the surface of a seed and thus lead to the switch of growth mode from asymmetric to symmetric. Our study suggests that symmetry reduction can only be initiated and retained by keeping the atom deposition at a rate slow enough to limit the number of initial nucleation sites on a seed but fast enough to beat the surface diffusion process.

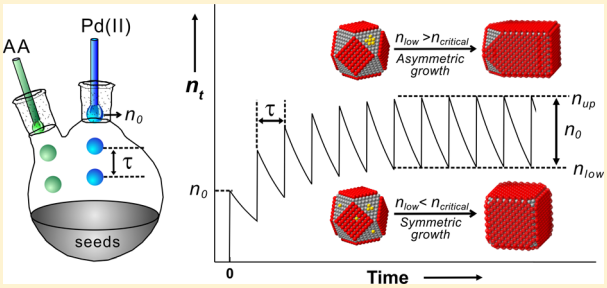

INTRODUCTION

There has been considerable interest in the chemical synthesis of noble-metal nanocrystals with specific shapes capable of enhancing their performance in various applications ranging from catalysis[1] to magnetism,[2] plasmonics,[3] electronics,[4] and medicine.[5] Although notable progress has been made in recent years with regard to the development of methods for controlling the shapes of noble-metal nanocrystals,[6] we still face challenges in producing nanocrystals with less symmetric shapes relative to the cubic lattice of a noble metal. When reduced in symmetry, the nanocrystals are anticipated with new properties to enrich fundamental studies and enable new applications. Notable examples include Au nanorods and Ag nanowires; both of them have found widespread use in applications related to plasmonics, electronics, and display.[3c,e,4d]

In contrast to an inorganic compound such as ZnO,[7] the crystal lattice of a noble metal takes a face-centered cubic (fcc) structure, with multiple facets equivalent to each other in terms of spatial arrangement and coordination number for the surface atoms. The high symmetry makes it inherently challenging to obtain noble-metal nanocrystals with shapes lower in symmetry than a cube. As a result, for noble-metal nanocrystals with a single-crystal structure, they often take a polyhedral (e.g., cubic, cuboctahedral, or octahedral) shape as confined by the cubic symmetry of the crystal lattice.[6] There are also reports for a number of noble metals, including Au,[8] Pd,[9] and Ag,[10] in which single-crystal nanostructures with a one-dimensional morphology (e.g., nanorods and nanobars) could be synthesized in the presence of bromide or other halide ions. In spite of extensive research, the exact mechanism responsible for the anisotropic, one-dimensional growth is still under debate. It is generally believed that the halide ions could somehow induce a faster growth rate along one of the three directions, leading to symmetry breaking and thus the formation of nanostructures with reduced symmetry relative to the cubic lattice.

With the use of a syringe pump to introduce the precursor solution, our group recently demonstrated an alternative strategy for breaking the cubic symmetry by manipulating the reaction kinetics involved in a seed-mediated growth process.[11,12] This strategy is effective not only for the generation of nanocrystals with reduced symmetry relative to the cubic lattice but also in avoiding self-nucleation.[13] In addition to the deposition on a seed, the newly formed atoms

Received: March 23, 2015
Published: May 5, 2015

DOI: 10.1021/jacs.5b03040
J. Am. Chem. Soc. 2015, 137, 6643−6652

Table 1. Summary of the Parameters Used for the Syntheses of Pd Nanocrystals via Seed-Mediated Growth

n_0	τ (s)	cuboctahedral seeds (μL)	cubic seeds (μL)	[Na_2PdCl_4] (mg/mL)	$Na_2PdCl_{4(aq)}$ vol (mL)	injection rate (mL/h)	results (Figure)
4.7	0.45	100		0.05	30.0	120.0	4b
4.7	0.9	100		0.05	30.0	60.0	4a
4.7	1.8	100		0.05	30.0	30.0	3a
11.7	1.8	100		0.125	12.0	30.0	3b
23.5	1.8	100		0.25	6.0	30.0	3c
23.5	3.6	100		0.25	6.0	15.0	4d
23.5	10.5	100		0.25	6.0	5.0	4e
70.5	1.8	100		0.75	2.0	30.0	3d
26.2	1.8		200	0.02	50.0	30.0	7a
26.2	10.5		200	0.02	50.0	5.0	7b

can self-nucleate and grow into nanocrystals concurrently if the concentration of atoms exceeds the threshold for self-nucleation, leading to the formation of nanocrystals with poorly controlled sizes and shapes. By using a syringe pump to introduce the precursor dropwise into a growth solution, the concentration of the newly formed atoms could be maintained at a level lower than the threshold to effectively suppress self-nucleation. More significantly, when the atoms initially formed in the growth solution are sufficiently smaller in number than the seed particles, heterogeneous nucleation can only occur at a limited number of the equivalent sites on a seed to trigger a growth pattern deviated from the cubic symmetry. For example, by controlling the injection rate of the precursor solution, we demonstrated that Ag or Au could be selectively deposited on different numbers of side faces (from one to six) of a Pd cubic seed to generate a nanocrystal with an asymmetric distribution for the deposited element.[11] When a similar strategy was applied to the growth of Ag on Ag cubic seeds, we obtained Ag nanocrystals with reduced symmetry relative to its cubic lattice, including rectangular bars and semitruncated octahedra.[12] Despite these successful demonstrations, it should be pointed out that all these studies were based on trial-and-error manipulation of the experimental parameters due to the lack of a mechanistic understanding and quantitative control. It is highly desired to have a quantitative understanding of the symmetry reduction phenomenon, especially with regard to the relationship between the growth mode and the reaction kinetics involved in seed-mediated growth.

Herein, we report a quantitative study of the symmetry reduction phenomenon involved in the seed-mediated growth of Pd nanocrystals. The experimental approach relies on the use of a syringe pump to introduce precursor ions dropwise into a growth solution containing well-defined seeds at a controllable rate to achieve a steady state for the number of precursor ions in the solution. On the basis of the reduction rate constant determined experimentally, the number of precursor ions in each drop (or the stock solution), and the duration of time between adjacent drops, we were able to obtain the kinetic information about a given synthesis, including the number of precursor ions in the growth solution as a function of the reaction time, as well as the lower and upper limits for the steady state. Our results indicate that the lower limit of precursor ions for the steady state plays a deterministic role in inducing symmetry reduction in a seed-mediated growth process. The lower limit has to be kept below a critical value in order to achieve asymmetric nucleation on a seed. At the same time, the lower limit has to be sufficiently high to ensure that the atoms are deposited at a rate faster than surface diffusion during the entire growth process. Otherwise, the surface diffusion of adatoms will eventually lead to the formation of a nanocrystal with symmetry similar to that of the seed. We note that previous studies only reported that a relatively slow atom deposition rate is critical to the induction of asymmetric growth.[11,12] The present work indicates that the atom deposition rate for asymmetric growth needs to be kept in a narrow range in order to induce and sustain the asymmetric growth mode. Most importantly, with the availability of reduction rate constant, it is possible, for the first time, to predict the experimental conditions (e.g., the injection rate and the precursor concentration) under which the growth mode will be switched from symmetric to asymmetric and vice versa.

EXPERIMENTAL SECTION

Chemicals and Materials. Ethylene glycol (EG) was purchased from J.T. Baker. Sodium tetrachloropalladate(II) (Na_2PdCl_4), poly(vinylpyrrolidone) (PVP, $M_W \approx 55\,000$), L-ascorbic acid (AA), and potassium bromide (KBr) were purchased from Sigma-Aldrich. All chemicals were used as received without further purification. Deionized (DI) water with a resistivity of 18.2 MΩ·cm was used for all syntheses.

Measurement of the Kinetic Parameters. We derived the rate constant (k) by analyzing the concentration of Pd(II) ions remaining in the reaction solution at different time points through inductively coupled plasma mass spectrometry (ICP-MS). Specifically, 2.0 mL of an aqueous solution containing 100.0 mg of AA and 1.2 mg of KBr was mixed in a 20 mL glass vial and heated to 40 °C in an oil bath for 20 min under magnetic stirring. Next, 1.0 mL of an aqueous Na_2PdCl_4 solution (1.0 mg/mL) was quickly injected into the vial in one shot. An aliquot of 0.1 mL was sampled from the reaction solution at different time points using a glass pipet and immediately injected into 0.9 mL of aqueous KBr solution (500 mg/mL) to quench the reduction reaction. The solution was then centrifuged at 55 000 rpm for 40 min to precipitate out all the Pd nanocrystals, leaving behind Pd(II) ions in the supernatant. Subsequently, the supernatant was collected and further diluted with 1% (v/v) aqueous HNO_3 solution to a level of 100 ppb for ICP-MS analysis. The concentrations of Pd(II) ions obtained at different time points were then used to determine the rate constant (k) by performing a linear regression fit to the plot of ln[Pd(II)] versus reaction time, with the slope of the regression line equal to $-k$. When the temperature was fixed, the rate constant could be used to calculate the instantaneous concentrations of the Pd(II) ions as a function of reaction time for all the seed-mediated growth experiments conducted in the present work.

Synthesis of the 4.5 nm Pd Cuboctahedral Seeds. The Pd cuboctahedra to be used as seeds for overgrowth were prepared using a recently reported protocol based on polyol reduction.[14] In a typical synthesis, 30 mg of PVP and 2.0 mL of EG were mixed in a 20 mL glass vial, and the mixture was heated to 160 °C under magnetic stirring. Next, 15.5 mg of Na_2PdCl_4 was dissolved in 1.0 mL of EG and added into the above mixture in one shot using a pipet. The reaction was allowed to proceed for 2 h. After centrifugation at 55 000 rpm and

DOI: 10.1021/jacs.5b03040
J. Am. Chem. Soc. 2015, 137, 6643−6652

being washed with ethanol and water three times, the Pd cuboctahedral seeds were redispersed in 3 mL of water.

Synthesis of the 10 nm Pd Cubic Seeds. The 10 nm Pd cubic seeds were prepared using a previously reported protocol.[15] In a typical synthesis, an 8 mL aqueous solution containing 105 mg of PVP, 60 mg of AA, and 300 mg of KBr was added into a 20 mL glass vial and heated at 80 °C for 5 min. Next, a 3 mL aqueous solution containing 57 mg of Na_2PdCl_4 was added in one shot under magnetic stirring. The reaction was allowed to proceed at 80 °C for 3 h. The product was collected by centrifugation at 16 000 rpm, washed with water three times, and redispersed in 11 mL of water.

Seed-Mediated Growth of Pd Nanocrystals. Table 1 shows a summary of the parameters used for the syntheses of Pd nanocrystals by seed-mediated growth. In a standard synthesis, an aqueous solution containing Na_2PdCl_4 (1.5 mg) and KBr (0.4 mg/mL) and another aqueous solution containing KBr (0.4 mg/mL) and AA (66.7 mg/mL) were introduced simultaneously using two syringe pumps into 3 mL of the growth solution—an aqueous suspension containing the seeds (0.1 mL for the 4.5 nm cuboctahedral seeds or 0.2 mL for the 10 nm cubic seeds), 100 mg of AA, 10 mg of PVP, and 1.2 mg of KBr in a 50 mL two-neck, round flask heated at 40 °C under magnetic stirring. For each drop of the precursor solution generated using a syringe pump at an injection rate of 30 mL/h, it had a volume of 0.015 mL. The concentration of the precursor solution was varied between syntheses to access a broad range of values for the initial number (n_0; see Results and Discussion for the definition) of the Pd(II) ions contained in each drop (see Table 1). After a specific amount of the precursor solution had been introduced, the growth was allowed to proceed for another 5 min and the product was then collected by centrifugation at 13 200 rpm, followed by washing with water three times.

Analysis of the Growth Mode. Our classification of the growth mode is based on the degree of symmetry for the resultant Pd nanocrystals. In analyzing the Pd nanocrystals by transmission electron microscopy (TEM) imaging, we defined the perfect nanocubes with O_h symmetry as the products of *symmetric growth*. In comparison, those nanocrystals with elongation along one or more directions (e.g., nanobars) and thus reduction in symmetry relative to a perfect cube were defined as the products of *asymmetric growth*. Specifically, the aspect ratio (length divided by width) of each particle was derived from TEM images. We then defined an aspect ratio of 1.1 as the borderline between *symmetric* and *asymmetric* growth. The histogram distributions of symmetric and asymmetric structures were obtained by counting 150 single-crystal particles in each sample, with the twinned particles being excluded from the analysis.

Characterizations. TEM images were taken using a Hitachi HT7700 microscope operated at 120 kV. The sample for TEM analysis was prepared by drying a drop of the nanocrystal suspension on a carbon-coated copper grid under ambient conditions. The concentration of Pd(II) precursor in the reaction solution was measured using an inductively coupled plasma mass spectrometer (NexION 300Q, PerkinElmer).

RESULTS AND DISCUSSION

Kinetic Parameters for the Reduction of a Pd(II) Precursor by AA. To quantitatively understand the effects of reaction kinetics on the transition from a symmetric to an asymmetric growth mode, it is necessary to tightly control the reduction rate for the Pd(II) precursor and thus the deposition rate for the resultant atoms. As the reduction of a salt precursor generally follows a second-order rate law due to the involvement of collision and electron transfer between a precursor ion and a reductant molecule, the reduction rate is expected to be directly proportional to the concentrations of both reagents.[16] Herein, we further achieved a pseudo-first-order rate law by supplying the reducing agent (i.e., AA in the present work) in great excess relative to the precursor. The excess amount of reducing agent in the system not only ensures a pseudo-first-order rate but also enables quick reduction of the Pd(II) precursor ions into Pd(0) atoms. Under this assumption, the rate law can be expressed as

$$r = k'[\mathrm{AA}][\mathrm{Pd(II)}] = k[\mathrm{Pd(II)}] \quad (1)$$

where k is the combined rate constant.

The combined rate constant can be obtained by plotting the instantaneous concentration of the Pd(II) precursor remaining in the reaction solution as a function of the reaction time.[17] Unlike a polyol synthesis conducted at an elevated temperature,[14,17] the strong reducing power of AA at room temperature makes it difficult to quench the reduction reaction in the current study by quickly cooling the reaction solution. Thanks to the high stability of $PdBr_4^{2-}$,[18] we found that the Pd(II) precursor can be prevented from being reduced by AA at room temperature for a relatively long period of time up to at least 60 min by adding a highly concentrated KBr solution (500 mg/mL) into the reaction solution. To validate the effectiveness of this quenching procedure, we conducted a control experiment in which an aqueous Na_2PdCl_4 solution (1.0 mg/mL) was injected into another aqueous solution containing both AA (33.3 mg/mL) and KBr (500 mg/mL) at 40 °C. Aliquots were then sampled from the solution for measuring the concentrations of Pd(II) ions by ICP-MS analysis. Figure 1a shows a plot of the concentration of Pd(II) ions remaining in the solution as a function of time, indicating that essentially no Pd(II) was reduced by AA when there was a great excess of Br^- ions in the solution even after they had been mixed for 60 min. We then applied this method to measure the reaction kinetics involving the reduction of the Pd(II) precursor by AA at 40 °C in an aqueous solution. Figure 1b shows a plot of $\ln[\mathrm{Pd(II)}]_t$ as a function of reaction time, indicating that the reduction indeed occurred as a first-order reaction with respect to the Pd(II) precursor. From the linear plot, we obtained a combined rate constant of 0.635 s^{-1} for the reduction of the Pd(II) precursor by AA at 40 °C. It should be pointed out that the actual Pd(II) precursor involved in the reduction could be a mixed-ligand complex (i.e., $PdCl_xBr_{4-x}^{2-}$, x = 1, 2, and 3) due to the rapid ligand exchange between $PdCl_4^{2-}$ and Br^- and that the exact composition is determined by the relative molar ratio of Cl^- to Br^- in the reaction solution.[18c] In the present work, we added an excess amount of KBr into the reaction solution to ensure that the Pd(II) ions were essentially in the form of $PdBr_4^{2-}$ due to a complete ligand exchange and a fixed composition for the Pd(II) precursor for all the seed-mediated syntheses described below.

It should be pointed out that some species other than Pd(II) ions, such as ultrafine particles and clusters (i.e., the nuclei), might remain in the supernatant because it might be difficult to sediment them by centrifugation. As a consequence, ICP-MS analysis of the supernatant might not reflect the true concentration of the precursor. However, giving their high activity and the absence of a colloidal stabilizer (PVP) in the kinetic measurements, the concentration of Pd ultrafine particles and clusters should be extremely low in the reaction solution. Otherwise, they would readily grow or aggregate into larger particles. To address this potential issue, we conducted UV−vis and X-ray photoelectron spectroscopy (XPS) analysis to confirm the actual species in the supernatant. As shown in Supporting Information Figure S1, the UV−vis spectrum of the supernatant exhibits the same absorption features as the precursor solution, confirming that the supernatant only contained the unreacted precursor ions. The absence of a continuous band in the visible region, which is typically

DOI: 10.1021/jacs.5b03040
J. Am. Chem. Soc. 2015, 137, 6643−6652

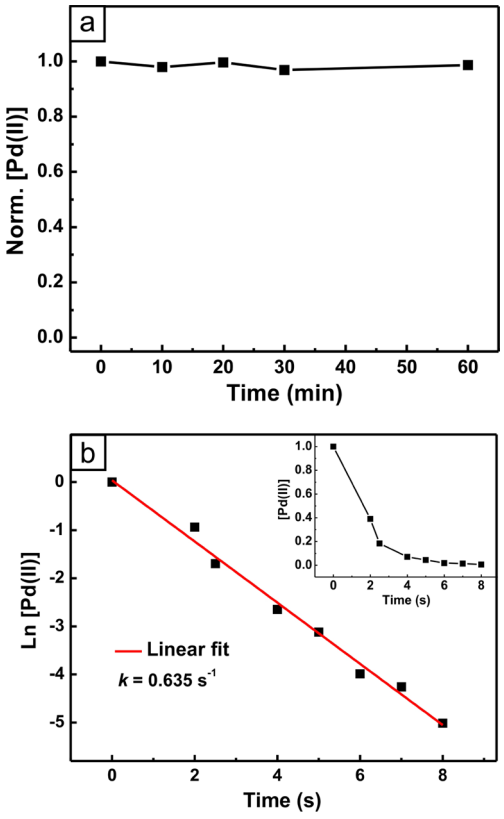

Figure 1. (a) ICP-MS analysis of the concentration of Pd(II) ions remaining in the reaction solution at different time points of a control experiment, indicating that the reduction of Pd(II) ions could be effectively quenched in the presence of Br^- ions at a concentration of 4.2 M (or 500 mg/mL in terms of KBr). (b) Plot of ln[Pd(II)] as a function of reaction time, giving a straight line with a slope that equals $-k$. The inset shows the concentration of Pd(II) ions remaining in the reaction solution as a function of reaction time. Note that the concentrations used in the plot were normalized to the initial concentration.

associated with the absorption/scattering of Pd nanocrystals, also suggests that there was essentially no detectable amount of Pd ultrafine particles or clusters in the supernatant. We also used the UV–vis method to derive the reduction kinetics by recording the absorption spectra of the supernatants obtained at different stages of a standard synthesis and determine the concentration of Pd(II) ions using a calibration curve. As shown in Figure S2, there is good agreement between the data obtained using the UV–vis and ICP-MS methods. The absence of Pd(0) species in the supernatant was further confirmed by XPS analysis (Figure S3). At least, it can be claimed that the concentration of Pd(0) species was below the detection limit of XPS and can thus be neglected in analyzing the reduction kinetics. Taken together, we believe that it is reasonable to exclude the possible errors arising from the negligible amount of Pd(0) species present in the supernatant during the measurement of reduction kinetics by ICP-MS.

Kinetic Analysis of Seed-Mediated Growth under the Dropwise Addition of a Precursor. Figure 2a shows a schematic illustration of the experimental approach used in the present study, where two aqueous solutions containing the Pd(II) precursor and AA (a reducing agent), respectively, are simultaneously injected with a controlled rate from two syringe pumps into an aqueous suspension containing the seeds, KBr (a

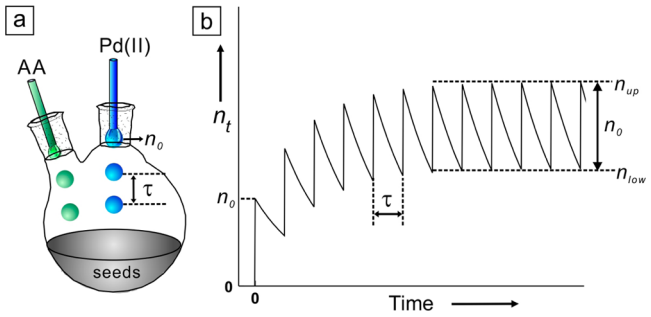

Figure 2. (a) Schematic illustration of the experimental setup used for seed-mediated growth with the dropwise addition of a precursor solution. (b) Plot showing the instantaneous number of Pd(II) ions (the precursor) in the growth solution (n_t) as a function of the reaction time (t), the duration of time between adjacent drops (τ), and the number of precursor ions contained in each drop (n_0). After the introduction of the first few drops, n_t will reach a steady state defined by an upper limit (n_{up}) and a lower limit (n_{low}). Note that the values of n_t, n_0, n_{up}, and n_{low} are all normalized to the number of seeds in the growth solution.

capping agent) and PVP (a colloidal stabilizer). Several experimental parameters, including the number of the Pd(II) precursor ions in each drop (n_0) and the duration of time between adjacent drops (τ), can be manipulated by changing the precursor concentration and tuning the injection rate, respectively, to tailor the reaction kinetics.

Given that the fraction of the total amount of precursor ions that will be reduced per unit time is independent of the initial precursor amount (or concentration) for a first-order reaction, the consumption of precursor from each drop can be derived separately. Mathematically, the total number of Pd(II) precursor ions remaining in the growth solution at time t can be expressed as a sum of contributions from all drops added up to this time point:

$$n_t = n_0 e^{-kt} + n_0 e^{-k(t-\tau)} + n_0 e^{-k(t-2\tau)} + \ldots + n_0 e^{-k(t-N\tau)} = \frac{n_0 e^{-kt} \times (1 - (e^{k\tau})^{N+1})}{1 - e^{k\tau}} \quad (2)$$

where n_t represents the instantaneous number of the Pd(II) precursor ions in the reaction solution; n_0 is the number of the Pd(II) precursor ions in each drop (i.e., in the stock solution); k is the combined rate constant derived from the ICP-MS analysis; t is the reaction time; τ is the duration of time between adjacent drops, and N is the total number of drops added into the solution up to time t. For the purpose of simplicity, here we normalized the numbers of the Pd(II) ions, both n_0 and n_t, to the number of seed particles in the growth solution, which was determined through a combination of TEM imaging and ICP-MS analysis.

When the precursor and the reducing agent for a seed-mediated growth process are fixed, the instantaneous number of the Pd(II) ions at different time points can be calculated using eq 2 for any pair of n_0 and τ. Figure 2b shows a generic plot for the instantaneous number of the Pd(II) ions in the growth solution as a function of the reaction time. If the duration of time (τ) between adjacent drops is sufficiently long, most of the Pd(II) ions will have been reduced to Pd(0) atoms and thus depleted from the growth solution before the next drop is introduced. In comparison, if the duration of time is relatively short, not all of the Pd(II) ions will be reduced before

DOI: 10.1021/jacs.5b03040
J. Am. Chem. Soc. 2015, 137, 6643–6652

the next drop is introduced, and the precursor ions will be gradually accumulated in the growth solution as the number of drops is increased. In this case, after a few drops, the instantaneous number (n_t) of the precursor ions will reach a steady state, in which it only fluctuates between a lower limit (n_{low}) and a upper limit (n_{up}). Specifically, each time a drop of the precursor solution is introduced during the steady state, the number of the precursor ions will quickly increase from n_{low} to n_{up}, followed by an exponential decay from n_{up} to n_{low} until the next drop is introduced. The difference between n_{up} and n_{low} simply equals n_0. The values of n_{up} and n_{low} can be easily calculated using eqs 3 and 4:

$$n_{up} = \frac{n_0}{1 - e^{-k\tau}} \quad (3)$$

$$n_{low} = \frac{n_0 \cdot e^{-k\tau}}{1 - e^{-k\tau}} \quad (4)$$

For the seed-mediated growth involving one-shot injection of the precursor solution,[14,19] the number of the precursor ions typically shows a drastic decrease during the course of growth. In comparison, the use of a syringe pump provides an opportunity to add the precursor solution dropwise and thereby enable us to maintain the precursor concentration in a steady state. As the reduction rate is directly proportional to the number of precursor ions in a pseudo-first-order reaction, the steady state enabled by the dropwise injection of precursor ions allows us to tightly control the reduction rate and thereby the atom deposition rate within a narrow range. In this way, we were able to achieve a quantitative understanding of the correlation between the growth mode and the reaction kinetics in a seed-mediated growth process.

The Role Played by the Number of Pd(II) Precursor Ions in Each Drop (n_0). To understand the role of n_0 in controlling the shape of Pd nanocrystals derived from seed-mediated growth, we conducted a set of experiments with different precursor concentrations. As reported in previous studies, a relatively low concentration for the precursor was required in order to induce asymmetric growth.[11,12] Unlike conventional seed-mediated growth, where thousands of precursor ions per seed are introduced into the growth solution for each drop (i.e., $n_0 > 10^3$),[20] we set n_0 to a much smaller number between 4.7 and 70.5 in the present work to achieve asymmetric growth. Initially, we focused on the growth of Pd on single-crystal Pd cuboctahedral seeds with an average size of 4.5 nm (Figure S4) in the presence of Br^- ions. Due to the preferential capping of Pd(100) surface by the Br^- ions,[21] it is expected that the introduction of Br^- ions will alter the order of surface free energies between different facets and thus facilitate the formation of Pd nanocubes enclosed by {100} facets. Since the degree of symmetry of the resultant Pd nanocrystals reflects the mode of growth during a seed-mediated growth process, we used TEM imaging to analyze the shape of particles in the product (see Figures S5 and S6 for details). Figure 3 shows TEM images of the resultant Pd nanocrystals. In addition to perfect nanocubes, the products also contained nanobars where one of the directions was elongated and thus the cubic symmetry was reduced, suggesting the involvement of both symmetric and asymmetric modes during the growth. Specifically, the proportion of cubic structures showed a negative correlation with n_0. For example, when n_0 was an extremely small number (4.7), the majority (78%) of nanocrystals in the final product was perfect nanocubes with

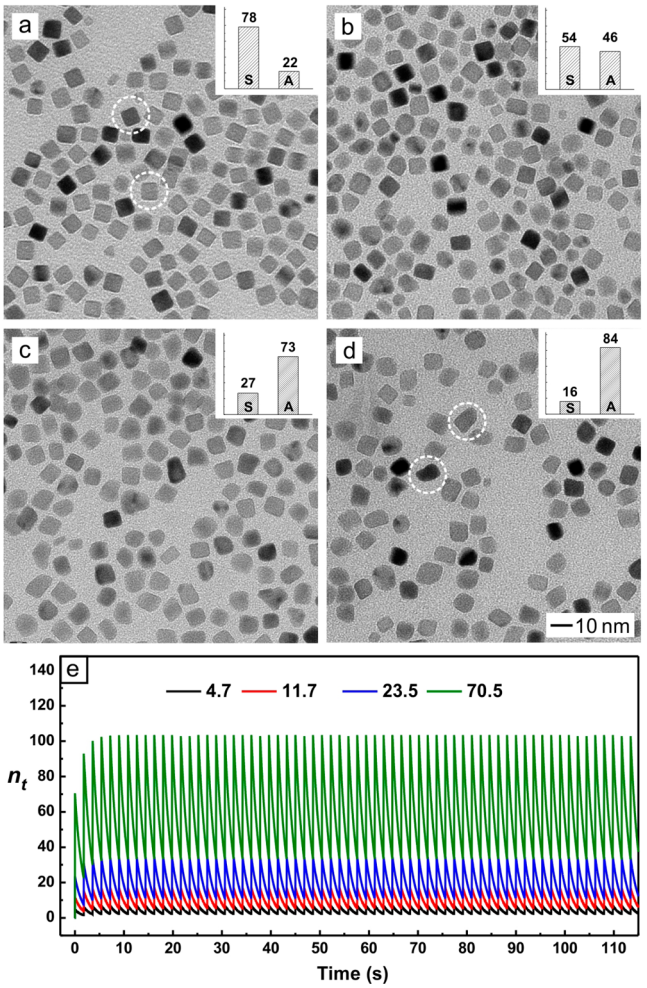

Figure 3. Controlling the mode of growth by changing the initial concentration of the precursor: (a–d) TEM images of Pd nanocrystals obtained by introducing the Pd(II) precursor solutions with different concentrations at an injection rate of 30 mL/h (τ = 1.8 s). The numbers of Pd(II) precursor ions contained in each drop (n_0, normalized to the number of seeds in the growth solution) were (a) 4.7, (b) 11.7, (c) 23.5, and (d) 70.5. The inset in each panel shows a histogram distribution of the nanocrystals with symmetric (S) and asymmetric (A) structures, respectively. (e) Simulated numbers of precursor ions as a function of the reaction time. The circles in (a) indicate the products of *symmetric growth*, and the circles in (d) mark the products of *asymmetric growth*.

a symmetry consistent with the lattice (Figure 3a). With the increase of n_0, the products were gradually transformed from perfect nanocubes to less symmetric, elongated nanocubes (e.g., nanobars). As shown in Figure 3b–d, the percentage of perfect nanocubes in the products decreased from 78% to 54, 27, and 16% as n_0 was increased from 4.7 to 11.7, 23.5, and 70.5, demonstrating a transition of the growth mode. In addition, we note that there were a few particles with uncommonly small sizes compared to the others in the TEM images, indicating that homogeneous nucleation was not completely suppressed, possibly due to the transient, local high concentration of precursor ions when each drop of precursor is added into the growth solution. However, considering that the majority of particles in the product was still grown from seeds, we believe that it was mostly based on heterogeneous nucleation and thus the minor self-nucleation process should have no impact on the overall growth mode of a synthesis.

DOI: 10.1021/jacs.5b03040
J. Am. Chem. Soc. 2015, 137, 6643–6652

Because the value of n_0 will affect the reaction kinetics, we hypothesize that the change in growth modes can be attributed to the variation of instantaneous precursor ion number (n_t) in the steady state. In order to quantitatively study the effect of the number of precursor ions supplied by each drop on the growth mode, we simulated the reaction kinetics under different values of n_0 using eq 2. As shown in Figure 3e, the number of precursor ions in the growth solution reached a steady state after the first few drops. Specifically, different values of n_0 resulted in steady states characterized by different ranges of n_{up} and n_{low}. For example, in the case of n_0 = 4.7, the fluctuation was confined to the range of 2.2 (n_{low}) to 6.9 (n_{up}). In contrast, when n_0 was increased to 70.5, the values of n_{low} and n_{up} increased to 33 and 103.5, respectively. These results indicate that there was a transition from symmetric growth to asymmetric growth when the values of the precursor ions involved in the steady state were increased.

The Role Played by the Duration of Time between Adjacent Drops (τ). In the second set of experiments, we adjusted τ by tuning the injection rate of precursor solution while keeping all other experimental parameters, including n_0 and reaction temperature, the same as the standard procedure. Based on eq 2, the value of n_t in the growth solution has a negative correlation with τ. Therefore, it is expected that shortening the duration of time between adjacent drops will increase the values of n_{up} and n_{low} in the steady state. Figure 4a,b shows TEM images of Pd nanocrystals synthesized using the protocol with n_0 = 4.7, the same as in Figure 3a except that the durations of time between adjacent drops were shortened from 1.8 to 0.9 and 0.45 s, respectively. The majority of product gradually changed from perfect cubes to elongated cubes with reduction in symmetry as the duration of time was decreased. Specifically, an analysis of the corresponding products indicates that the percentage of perfect nanocubes dropped from 78 to 36% as the duration of time was shortened from 1.8 to 0.9 s and eventually reached 18% when a very short duration of 0.45 s was involved. The simulation of reaction kinetics given in Figure 4c confirms the increase in n_{up} and n_{low} for the steady state as the duration of time between adjacent drops was shortened.

We also applied a similar analysis to the synthesis shown in Figure 3c, where n_0 was set to 23.5 and the product was dominated by elongated cubes with reduced symmetry relative to the cubic lattice. As shown in Figure 4d, when the duration of time between adjacent drops was increased from 1.8 to 3.6 s, the proportion of cubic structures increased from 27 to 76%. Finally, it reached 88% when the duration was increased to 10.5 s, and the product mainly contained perfect cubes (Figure 4e). Due to the relatively long duration of time in the case of τ = 10.5 s, most of the precursor should have been depleted before the next drop was introduced, resulting in an extremely low value of 0.03 for the n_{low} in the steady state. This significant change to the morphology of the resultant nanocrystals can also be attributed to the change in reaction kinetics, as documented in Figure 4f, where the increase in τ effectively decreased the values of n_{up} and n_{low} and thereby slowed the overall atom deposition rate.

Correlation between Growth Mode and n_{low}. It is now clear that the switching of seed-mediated growth from a symmetric to an asymmetric mode can be achieved using two different methods that involve variations to the number of precursor ions in each drop (n_0) and/or the duration of time between adjacent drops (τ). To achieve a better understanding

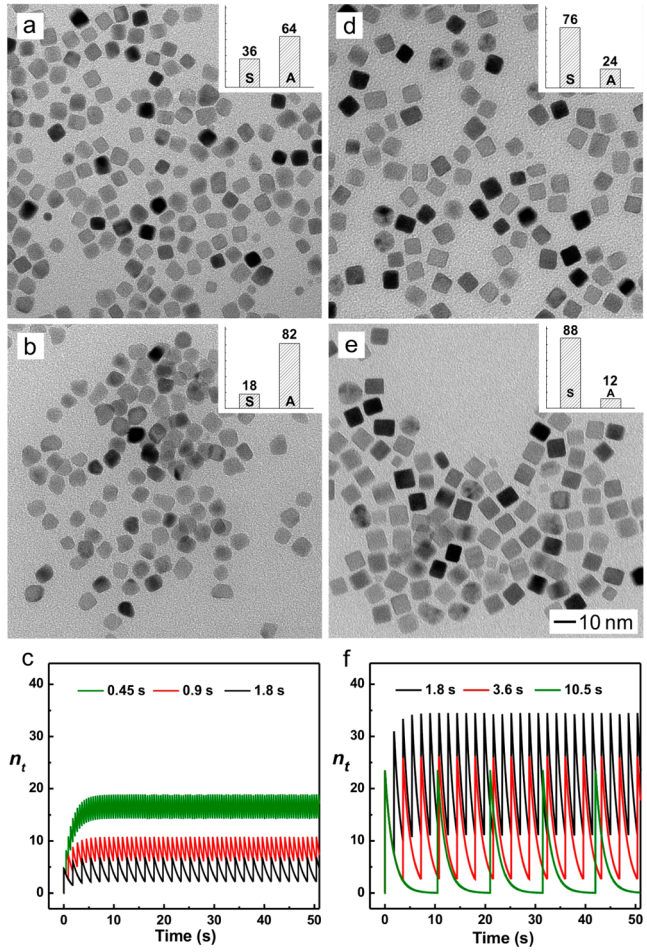

Figure 4. Controlling the mode of growth by varying the precursor injection rate to change the duration of time between adjacent drops: (a,b) TEM images of Pd nanocrystals prepared by injecting a Na_2PdCl_4 solution of 0.1 mg/mL, where the number of Pd(II) precursor ions in each drop (n_0, normalized to the number of seeds) was 4.7. The durations of time between adjacent drops (τ) were (a) 0.9 s and (b) 0.45 s. (d,e) TEM images of Pd nanocrystals obtained by injecting a Na_2PdCl_4 solution of 0.5 mg/mL, corresponding to a value of 23.5 for n_0. The values of τ were (d) 3.6 s and (e) 10.5 s. The inset in each TEM image shows a histogram distribution of the symmetric and asymmetric structures. (c,f) Simulated numbers of precursor ions as a function of the reaction time.

toward the explicit mechanism, we made a side-by-side comparison of the results and the reaction kinetics from the aforementioned two methods in an effort to single out a key factor responsible for the switching of the growth mode. Interestingly, both methods show a common transition point around n_{low} = 8 that separates the two distinctive growth modes in the current system.

Because n_{low} is a function of both n_0 and τ, a curve representing a specific value of n_{low} can be made in a plot of n_0 versus τ. As shown in Figure 5a, the solid line indicates the boundary of n_{low} = 8, with the left side being greater than 8 and the rest being less than 8. By correlating the values of n_{low} and the proportions of symmetrically reduced particles under different conditions, a transition between the two growth modes can be clearly observed along the boundary (Figure 5b). Specifically, when n_{low} was greater than 8 in a given synthesis, the majority of nanocrystals in the product would be characterized as elongated nanocubes with reduced symmetry,

DOI: 10.1021/jacs.5b03040
J. Am. Chem. Soc. 2015, 137, 6643−6652

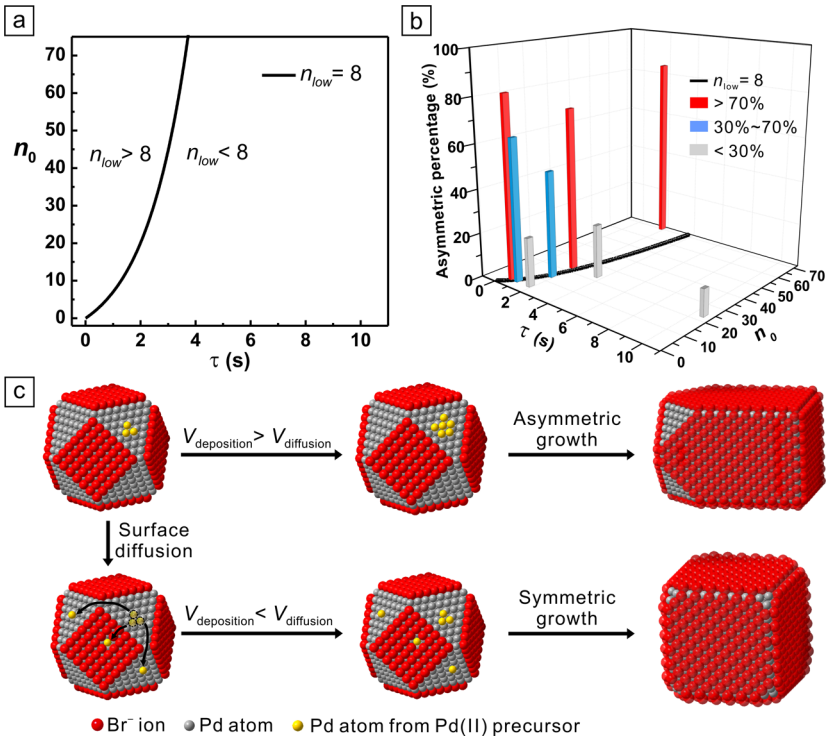

Figure 5. (a) Plot showing n_{low} (the lower limit of the number of precursor ions in the steady state of a synthesis) as a function of n_0 (the number of precursor ions contained in each drop) and τ (the duration of time between adjacent drops). (b) Bar chart showing the percentages of asymmetric structures formed under different reaction conditions, suggesting a transition of growth from an asymmetric mode to a symmetric mode when n_{low} was reduced to pass a critical value around 8. Note that the values of both n_{low} and n_0 are all normalized to the number of seeds in the growth solution. (c) Schematic illustration showing the effect of reaction kinetics and surface diffusion on the growth mode of a Pd cuboctahedral seed.

indicating that asymmetric growth dominated in this region. In comparison, when n_{low} was less than 8, the growth would be switched to symmetric mode, together with the formation of perfect cubes. For the region close to the boundary, the resultant product would be a mixture of nanocrystals with symmetric and asymmetric structures at approximately equal proportions, demonstrating the coexistence of both growth modes under these conditions.

Figure 5c schematically illustrates a plausible mechanism responsible for the growth modes and the two possible overgrowth patterns for a cuboctahedral seed. Since the {100} facets of a Pd cuboctahedral seed are blocked by Br^- ions through chemisorption,[20] the initially formed Pd atoms should be preferentially deposited onto the Pd{111} facets to generate kinks on these surfaces with a relatively higher surface energy that can serve as the active sites to promote the following atom deposition. However, the limited number of resultant Pd atoms supplied from the first few drops can only activate some of the eight {111} facets on each seed. Upon the subsequent introduction of more precursor solution, the deposition of the newly formed atoms will be largely limited to these activated sites, resulting in asymmetric growth for the cuboctahedral seed. Once deposited, there is a probability for the adatoms to migrate to adjacent {111} facets of the same seed through surface diffusion. As such, the initially deposited atoms at the kink sites will be able to migrate to other {111} facets through surface diffusion once the diffusion rate becomes comparable to the atom deposition rate, eventually generating active sites on all of the eight {111} facets.

Combined together, we believe that the growth mode (or pattern) of a seed is governed by the ratio between the atom deposition rate ($V_{deposition}$) and the surface diffusion rate ($V_{diffusion}$). In order to limit the number of activated sites on the seed and achieve asymmetric growth, the atom deposition rate needs to be greater than the surface diffusion rate (i.e., $V_{deposition} > V_{diffusion}$). In contrast, if $V_{diffusion}$ is greater than $V_{deposition}$, all of the eight {111} facets can be activated to induce symmetric growth. When $V_{diffusion}$ and $V_{deposition}$ become comparable, the two growth modes will coexist and compete with each other. Consequently, some of the seeds will undergo symmetric growth while the other will follow asymmetric growth, resulting in a mixture of nanocrystals with different degrees of symmetry.

Based on the proposed mechanism, the correlation between growth mode and n_{low} can be understood from the following aspects. According to the pseudo-first-order rate law in eq 1, the reduction rate and thus the atom deposition rate are proportional to the instantaneous number of precursor ions (n_t) in the growth solution. Because n_t constantly varied in the range of n_{up} and n_{low} during a steady-state growth process, the corresponding atom deposition rate should fluctuate between a maximum value and a minimum value. In this case, as long as the minimum value is above the threshold required for inducing asymmetric growth, the entire seed-mediated growth process will be exclusively locked in the asymmetric mode.

Influence of Reaction Temperature on Surface Diffusion. Because surface diffusion is a thermally promoted process, it can be suppressed or enhanced by decreasing or increasing the reaction temperature, respectively.[21] Due to the strong reducing power of AA, the reduction rate of the Pd(II) precursor and $V_{deposition}$ for a given precursor concentration over the temperature ranging from 20 to 80 °C can be assumed

DOI: 10.1021/jacs.5b03040
J. Am. Chem. Soc. 2015, 137, 6643−6652

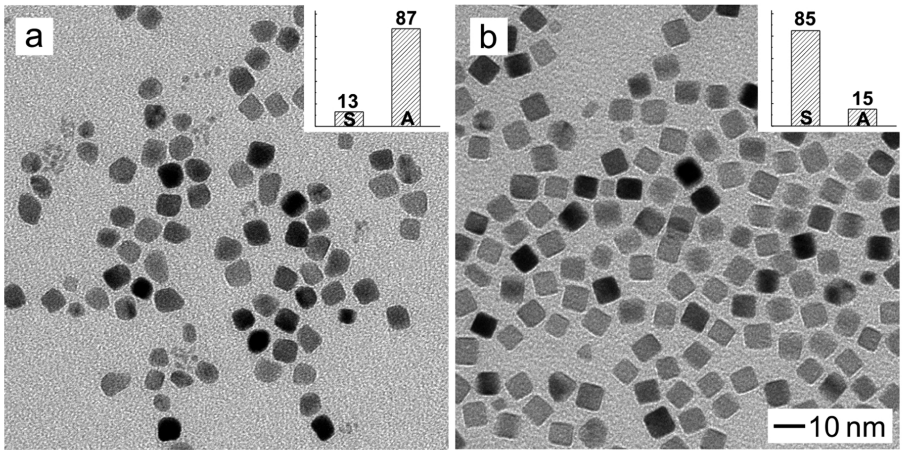

Figure 6. (a) TEM image of Pd nanocrystals prepared under the same conditions as in Figure 3a, except that the reaction temperature was set to 20 °C. (b) TEM image of Pd nanocrystals prepared using the same conditions as in Figure 3d, except that the reaction temperature was set to 80 °C. The inset in each TEM image shows a histogram distribution of the symmetric and asymmetric structures.

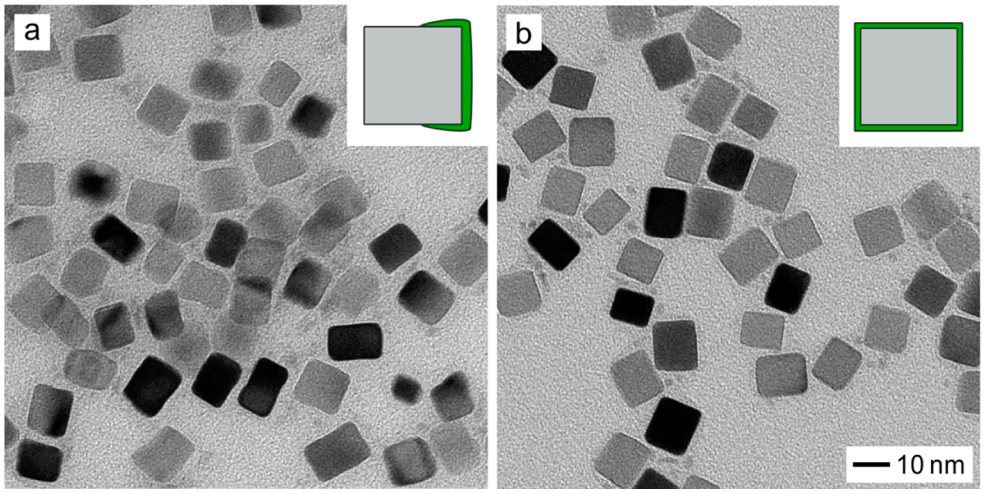

Figure 7. TEM images of the two distinctive types of Pd nanocrystals that were obtained via the overgrowth of 10 nm cubic seeds under (a) asymmetric and (b) symmetric modes. The number of Pd(II) precursor ions (n_0, normalized to the number of seeds) in each drop was 26, and the durations between adjacent drops (τ) were 1.8 and 10.5 s for asymmetric and symmetric modes, respectively. The insets show 2-D projection models of the nanocrystals corresponding to the TEM images, where the gray and green colors represent the seed and the newly deposited Pd, respectively.

to be more or less on the same level as in the standard procedure (40 °C). As such, manipulating the reaction temperature allows us to easily adjust the $V_{diffusion}$ involved in the growth process. Based on our proposed mechanism, any variation to $V_{diffusion}$ as caused by reaction temperature should provide another way to reverse the order of $V_{diffusion}$ and $V_{deposition}$ and thus to switch the growth mode.

We conducted an experiment by decreasing the reaction temperature to 20 °C while keeping other reaction parameters the same as in Figure 3a. Different from the perfect nanocubes obtained at 40 °C (see Figure 3a), elongated cubes with reduced symmetry became the major product, as shown in Figure 6a, when the temperature was decreased to 20 °C, implying that the reduced $V_{diffusion}$ promoted the switching of the growth mode. A similar transition was also observed in another experiment conducted under the same condition as in Figure 3d, except that the temperature was increased from 40 to 80 °C. As expected, the significant increase in surface diffusion at 80 °C changed the order of rates to $V_{diffusion} > V_{deposition}$, thus switching the growth from an asymmetric mode to a symmetric mode, as confirmed by the formation of perfect nanocubes in Figure 6b. Taken together, these results suggest that, in addition to the manipulation of atom deposition rate ($V_{deposition}$), the growth mode of a seed can also be controlled by varying the surface diffusion rate ($V_{diffusion}$).

Extension from 4.5 nm Cuboctahedral Seeds to 10 nm Cubic Seeds. We also extended the strategy to another type of seeds by replacing the 4.5 nm cuboctahedra used in the standard procedure with 10 nm Pd nanocubes as the seeds. It should be pointed out that the Pd cubic seeds with an average side length of 10 nm had a slightly reduced cubic shape as one of the directions was slightly elongated, as shown by the rectangular projection in the TEM image (Figure S7). For the purpose of simplicity, we refer to them as 10 nm cubic seeds. Based on our quantitative analysis, we conducted a set of experiments to demonstrate how the growth mode of such cubic seeds can be switched between symmetric and asymmetric modes. Figure 7a shows a TEM image of the resultant Pd nanocrystals synthesized under the condition where the growth was dominated by asymmetric mode (i.e., with $V_{deposition} > V_{diffusion}$). It can be seen that the cubic seeds underwent asymmetric growth and the newly formed Pd atoms

DOI: 10.1021/jacs.5b03040
J. Am. Chem. Soc. 2015, 137, 6643−6652

were largely deposited on some of the corners on a cubic seed. Basically, the Pd atoms were supposed to be deposited on the eight corners of a cubic seed because their side {100} faces were blocked by Br^- ions. However, due to the relatively small number of precursor ions, the initially formed Pd atoms were only deposited on a limited number of the corners upon the introduction of the first few drops. When the deposition rate was greater than the diffusion rate, the subsequently introduced atoms would be continuously deposited on the activated corners, leading to the formation of nanocrystals with a less symmetric structure relative to the cubic lattice. In comparison, when the duration of time between adjacent drops (τ) was extended to enable the switching of growth from asymmetric to symmetric modes, enlarged Pd nanocubes were obtained as the product. As shown in Figure 7b, the cubic symmetry of nanocubes was more or less retained during the overgrowth. In this case, $V_{diffusion}$ became greater than $V_{deposition}$, and thus the initially deposited atoms could migrate to other corners and even the side {100} facets through surface diffusion, leading to symmetric growth.

CONCLUSIONS

In summary, we have quantitatively analyzed the symmetry reduction phenomenon involved in the seed-mediated growth of Pd nanocrystals under the dropwise introduction of a precursor solution with the use of a syringe pump. The dropwise approach allowed for a tight control over the reduction rate and thus the achievement of a steady state (as defined by the upper and lower limits) for the number of precursor ions in the solution and a narrow range for the variations of atom deposition rate. Based on the reduction rate constant determined experimentally, we could predict the kinetics of a given synthesis, including the number of precursor ions in the growth solution as a function of time, as well as the upper and lower limits of the steady state. Using Pd cuboctahedral seeds as an example, we have demonstrated the ability to switch the growth of a seed between symmetric and asymmetric modes by quantitatively tuning the experimental parameters such as the initial concentration of the precursor solution and the injection rate. Our analysis suggested that the switching of the growth mode was determined by the lower-limit number (n_{low}) of precursor ions in the steady state, which controlled the minimum rate responsible for the deposition of atoms onto a seed. When the first few drops of precursor solution were introduced, the resultant atoms could only be deposited on a limited number of equivalent sites on the surface of a seed to induce asymmetric growth if n_{low} was kept below a critical value. In order to maintain the asymmetric growth, the deposition of atoms needed to be kept at a faster pace than surface diffusion by controlling n_{low} above a value of eight for the Pd cuboctahedral seeds. In contrast, the seeds would take a symmetric growth mode when n_{low} was reduced to a level below eight by decreasing n_0 and/or extending τ. In this case, the migration of adatoms through surface diffusion could access other sites on the surface, switching the growth from asymmetric to symmetric mode. In addition to the manipulation of atom deposition rate, we could switch the growth mode of a seed by varying the reaction temperature to alter the surface diffusion rate. We believe that this work would greatly advance our mechanistic understanding of the symmetry reduction phenomenon commonly involved in the seed-mediated growth of nanocrystals and provide a guideline for rational design and synthesis of nanocrystals with less symmetric shapes than a cubic lattice.

ASSOCIATED CONTENT

Supporting Information

UV−vis spectra of the precursor solution, the reaction solution of a standard synthesis, and the supernatant and precipitate of a standard synthesis after separation via centrifugation. UV−vis spectra of the supernatants obtained at different stages of a standard synthesis. High-resolution Pd 3d XPS spectrum of the supernatant of a standard synthesis. TEM images of the 4.5 nm Pd cuboctahedral seeds and the 10 nm Pd cubic seeds. Aspect ratio histograms and enlarged TEM images of the samples shown in Figure 3, with all particles labeled as symmetric or asymmetric. The Supporting Information is available free of charge on the ACS Publications website at DOI: 10.1021/jacs.5b03040.

AUTHOR INFORMATION

Corresponding Author

*younan.xia@bme.gatech.edu

Notes

The authors declare no competing financial interest.

ACKNOWLEDGMENTS

This work was supported in part by a grant from the NSF (DMR-1215034) and start-up funds from the Georgia Institute of Technology.

REFERENCES

(1) (a) Moreno-Mañas, M.; Pleixats, R. *Acc. Chem. Res.* **2003**, *36*, 638−643. (b) Stamenkovic, V. R.; Fowler, B.; Mun, B. S.; Wang, G.; Ross, P. N.; Lucas, C. A.; Marković, N. M. *Science* **2007**, *26*, 493−497. (c) Lim, B.; Jiang, M.; Camargo, P. H.; Cho, E. C.; Tao, J.; Lu, X.; Zhu, Y.; Xia, Y. *Science* **2009**, *324*, 1302−1305. (d) Guo, S.; Zhang, S.; Sun, S. *Angew. Chem., Int. Ed.* **2010**, *52*, 8526−8544. (e) Zhang, H.; Watanabe, T.; Okumura, M.; Haruta, M.; Toshima, N. *Nat. Mater.* **2012**, *11*, 49−52.

(2) (a) Zeng, H.; Li, J.; Liu, J. P.; Wang, Z. L.; Sun, S. *Nature* **2002**, *420*, 395−398. (b) Seo, W. S.; Lee, J. H.; Sun, X.; Suzuki, Y.; Mann, D.; Liu, Z.; Terashima, M.; Yang, P. C.; McConnell, M. V.; Nishimura, D. G.; Dai, H. *Nat. Mater.* **2006**, *5*, 971−976. (c) Lu, A.-H.; Salabas, E. L.; Schüth, D. *Angew. Chem., Int. Ed.* **2007**, *46*, 1222−1244.

(3) (a) Cao, Y. C.; Jin, R.; Mirkin, C. A. *Science* **2002**, *297*, 1536−1540. (b) Ditlbacher, H.; Hohenau, A.; Wagner, D.; Kreibig, U.; Rogers, M.; Hofer, F.; Aussenegg, F. R.; Krenn, J. R. *Phys. Rev. Lett.* **2005**, *95*, 257403. (c) Burda, C.; Chen, X.; Narayanan, R.; El-Sayed, M. A. *Chem. Rev.* **2005**, *105*, 1025−1102. (d) Huang, X.; Tang, S.; Mu, X.; Dai, Y.; Chen, G.; Zhou, Z.; Ruan, F.; Yang, Z.; Zheng, N. *Nat. Nanotechnol.* **2011**, *6*, 28−32. (e) Rycenga, M.; Cobley, C. M.; Zeng, J.; Li, W.; Moran, C. H.; Zhang, Q.; Qin, D.; Xia, Y. *Chem. Rev.* **2011**, *111*, 3669−3712.

(4) (a) Sato, T.; Ahmed, H.; Brown, D.; Johnson, B. F. G. *J. Appl. Phys.* **1997**, *82*, 696−701. (b) Vanmaekelbergh, D. *Nature* **2009**, *4*, 475−476. (c) Talapin, D. V.; Lee, J.-S.; Kovalenko, M. V.; Shevchenko, E. V. *Chem. Rev.* **2010**, *110*, 389−458. (d) Hu, L.; Kim, H. S.; Lee, J.-Y.; Peumans, P.; Cui, Y. *ACS Nano* **2010**, *4*, 2955−2963.

(5) (a) Rosi, N. L.; Mirkin, C. A. *Chem. Rev.* **2005**, *105*, 1547−1562. (b) Yavuz, M. S.; Cheng, Y.; Chen, J.; Cobley, C. M.; Zhang, Q.; Rycenga, M.; Xie, J.; Kim, C.; Song, K. H.; Schwartz, A. G.; Wang, L. V.; Xia, Y. *Nat. Mater.* **2009**, *8*, 935−939. (c) Dreaden, E. C.; Mackey, M. A.; Huang, X.; Kang, B.; El-Sayed, M. A. *Chem. Soc. Rev.* **2011**, *40*, 3391−3404.

(6) (a) Ahmadi, T. S.; Wang, Z. L.; Green, T. C.; Henglein, A.; El-Sayed, M. A. *Science* **1996**, *272*, 1924−1926. (b) Park, J.; Joo, J.; Kwon,

DOI: 10.1021/jacs.5b03040
J. Am. Chem. Soc. 2015, 137, 6643−6652

S. G.; Jang, Y.; Hyeon, T. *Angew. Chem., Int. Ed.* **2007**, *46*, 4630−4660. (c) Tao, A. R.; Habas, S.; Yang, P. *Small* **2008**, *3*, 310−325. (d) Xia, Y.; Xiong, Y.; Lim, B.; Skrabalak, S. E. *Angew. Chem., Int. Ed.* **2009**, *48*, 60−103.
(7) (a) Kong, X. Y.; Ding, Y.; Yang, R.; Wang, Z. L. *Science* **2004**, *303*, 1348−1351. (b) Wang, Z. L.; Kong, X. Y.; Zuo, J. M. *Phys. Rev. Lett.* **2003**, *91*, 185502.
(8) (a) Nikoobakht, B.; El-Sayed, M. A. *Chem. Mater.* **2003**, *15*, 1957−1962. (b) Pérez-Juste, J.; Liz-Marzán, L. M.; Carnie, S.; Chan, D. Y. C.; Mulvaney, P. *Adv. Funct. Mater.* **2004**, *14*, 571−579. (c) Orendorff, C. J.; Murphy, C. J. *J. Phys. Chem. B* **2006**, *110*, 3990−3994.
(9) (a) Xiong, Y.; Cai, H.; Wiley, B. J.; Wang, J.; Kim, M. J.; Xia, Y. *J. Am. Chem. Soc.* **2007**, *129*, 3665−3675. (b) Sun, Y.; Zhang, L.; Zhou, H.; Zhu, Y.; Sutter, E.; Ji, Y.; Rafailovich, M. H.; Sokolov, J. C. *Chem. Mater.* **2007**, *19*, 2065−2070.
(10) (a) Wiley, B. J.; Chen, Y.; McLellan, J. M.; Xiong, Y.; Li, Z.-Y.; Ginger, D.; Xia, Y. *Nano Lett.* **2007**, *7*, 1032−1036. (b) Zhang, Q.; Moran, C. H.; Xia, X.; Rycenga, M.; Li, N.; Xia, Y. *Langmuir* **2012**, *28*, 9047−9054.
(11) (a) Zeng, J.; Zhu, C.; Tao, J.; Jin, M.; Zhang, H.; Li, Z.-Y.; Zhu, Y.; Xia, Y. *Angew. Chem., Int. Ed.* **2012**, *51*, 2354−2358. (b) Zhu, C.; Zeng, J.; Tao, J.; Johnson, M. C.; Schmidt-Krey, I.; Blubaugh, L.; Zhu, Y.; Gu, Z.; Xia, Y. *J. Am. Chem. Soc.* **2012**, *134*, 15822−15831.
(12) Xia, X.; Xia, Y. *Nano Lett.* **2012**, *12*, 6038−6042.
(13) (a) Habas, S. E.; Lee, H.; Radmilovic, V.; Somorjai, G. A.; Yang, P. *Nat. Mater.* **2007**, *6*, 692−697. (b) Zhang, H.; Li, W.; Jin, M.; Zeng, J.; Yu, T.; Yang, D.; Xia, Y. *Nano Lett.* **2011**, *11*, 898−903. (c) Wang, D.; Li, Y. *Adv. Mater.* **2011**, *23*, 1044−1060. (d) Langille, M. R.; Zhang, J.; Personick, M. L.; Li, S.; Mirkin, C. A. *Science* **2012**, *337*, 954−957.
(14) Wang, Y.; Xie, S.; Liu, J.; Park, J.; Huang, C. Z.; Xia, Y. *Nano Lett.* **2013**, *13*, 2276−2281.
(15) Jin, M.; Liu, H.; Zhang, H.; Xie, Z.; Liu, J.; Xia, Y. *Nano Res.* **2011**, *4*, 83−91.
(16) Luty-Błocho, M.; Pacławski, K.; Wojnicki, M.; Fitzner, K. *Inorg. Chim. Acta* **2013**, *395*, 189−196.
(17) Wang, Y.; Peng, H.-C.; Liu, J.; Huang, C. Z.; Xia, Y. *Nano Lett.* **2015**, *15*, 1445−1450.
(18) (a) Feldberg, S.; Klotz, P.; Newman, L. *Inorg. Chem.* **1972**, *11*, 2860−2865. (b) Dean, J. A. *Lange's Chemistry Handbook*, 15th ed.; McGraw-Hill Professional: New York, 1998. (c) Timoshkin, A. Y.; Kudrev, A. G. *Russ. J. Inorg. Chem.* **2012**, *57*, 1362−1970.
(19) (a) Niu, W.; Zhang, L.; Xu, G. *ACS Nano* **2010**, *4*, 1987−1996. (b) Jin, M.; Zhang, H.; Xie, Z.; Xia, Y. *Energy Environ. Sci.* **2012**, *5*, 6352−6357. (c) Gao, C.; Vuong, J.; Zhang, Q.; Liu, Y.; Yin, Y. *Nanoscale* **2012**, *4*, 2875−2878.
(20) Peng, H.-C.; Xie, S.; Park, J.; Xia, X.; Xia, Y. *J. Am. Chem. Soc.* **2013**, *135*, 3780−3783.
(21) Xia, X.; Xie, S.; Liu, M.; Peng, H.-C.; Lu, N.; Wang, J.; Kim, M. J.; Xia, Y. *Proc. Natl. Acad. Sci. U.S.A.* **2013**, *110*, 6669−6673.

DOI: 10.1021/jacs.5b03040
J. Am. Chem. Soc. 2015, 137, 6643−6652